Article

Cell Systems

Matched-Comparative Modeling of Normal and Diseased Human Airway Responses Using a Microengineered Breathing Lung Chip

Graphical Abstract

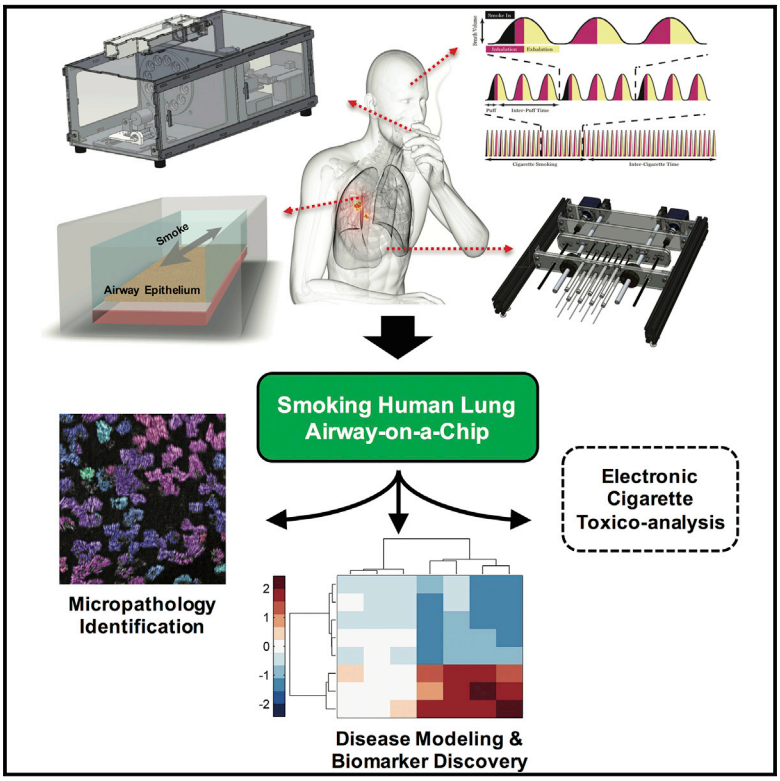

Authors

Kambez H. Benam, Richard Novak, Janna Nawroth, ..., Anthony Bahinski, Kevin K. Parker, Donald E. Ingber

Correspondence

don.ingber@wyss.harvard.edu

In Brief

Benam et al. describe a microengineered in vitro model system that permits analysis of the effects of whole smoke, from both conventional tobacco and electronic cigarettes, delivered under physiologically relevant flow conditions that mimic breathing on the pathophysiology of differentiated human mucociliated bronchiolar epithelium cultured in a microfluidic small airway-on-a-chip.

Highlights

- Smoking lung airway chip recapitulated clinical oxidative stress molecular profiles
- New smoke-induced ciliary micropathologies were identified
- This technology supported study of potential toxic effects of electronic cigarettes
- COPD-specific responses were reproduced in vitro and novel biomarkers were identified

Data Resources

GSE87098

Benam et al., 2016, Cell Systems *3*, 456–466
November 23, 2016
http://dx.doi.org/10.1016/j.cels.2016.10.003

CellPress

Cell Systems
Article

Matched-Comparative Modeling of Normal and Diseased Human Airway Responses Using a Microengineered Breathing Lung Chip

Kambez H. Benam,[1] Richard Novak,[1] Janna Nawroth,[1,2,5] Mariko Hirano-Kobayashi,[1,3] Thomas C. Ferrante,[1] Youngjae Choe,[1] Rachelle Prantil-Baun,[1] James C. Weaver,[1,2] Anthony Bahinski,[1] Kevin K. Parker,[1,2] and Donald E. Ingber[1,2,3,4,6,*]

[1]Wyss Institute for Biologically Inspired Engineering, Boston, MA 02115, USA
[2]Harvard John A. Paulson School of Engineering and Applied Sciences, Cambridge, MA 02139, USA
[3]Vascular Biology Program, Boston Children's Hospital, Boston, MA 02115, USA
[4]Department of Surgery, Harvard Medical School, Boston, MA 02115, USA
[5]Present address: Emulate, Inc., 27 Drydock Avenue, Boston, MA 02210, USA
[6]Lead Contact
*Correspondence: don.ingber@wyss.harvard.edu
http://dx.doi.org/10.1016/j.cels.2016.10.003

SUMMARY

Smoking represents a major risk factor for chronic obstructive pulmonary disease (COPD), but it is difficult to characterize smoke-induced injury responses under physiological breathing conditions in humans due to patient-to-patient variability. Here, we show that a small airway-on-a-chip device lined by living human bronchiolar epithelium from normal or COPD patients can be connected to an instrument that "breathes" whole cigarette smoke in and out of the chips to study smoke-induced pathophysiology in vitro. This technology enables true matched comparisons of biological responses by culturing cells from the same individual with or without smoke exposure. These studies led to identification of ciliary micropathologies, COPD-specific molecular signatures, and epithelial responses to smoke generated by electronic cigarettes. The smoking airway-on-a-chip represents a tool to study normal and disease-specific responses of the human lung to inhaled smoke across molecular, cellular and tissue-level responses in an organ-relevant context.

INTRODUCTION

Cigarette smoking is a common cause of lung disorders, and it is the primary risk factor for the development of chronic obstructive pulmonary disease (COPD), which is the third leading cause of death worldwide (Powell et al., 2013; Rennard and Drummond, 2015). Smoke-induced disease exacerbations represent one of the common causes for COPD patients to seek medical care (Sapey and Stockley, 2006). In addition, tobacco-related products such as electronic cigarettes (e-cigarettes) are drastically gaining popularity, but the biological impact of their emissions on lung is poorly characterized, and this is emerging as a potential health concern for regulatory agencies (Neilson et al., 2015; Rowell and Tarran, 2015). Neither small airway disease nor COPD exacerbations caused by cigarette smoke can be effectively modeled in animals (Adamson et al., 2011a; Vlahos and Bozinovski, 2014; Wright et al., 2008). Because commonly used laboratory animals (e.g., mice, rats) are obligate nose-breathers, their applicability for smoke exposure studies, either from conventional cigarettes or e-cigarettes, is also debatable. Culture systems have been developed to study the effects of smoke on human lung epithelium (Glader et al., 2006; Mathis et al., 2013; Mio et al., 1997; Mulligan et al., 2009); however, they are unable to reproduce physiological breathing air movements that are responsible for delivering smoke to the lung epithelium. Moreover, these models have predominantly focused on the toxicity of tobacco smoke exposure. While human clinical studies are the most direct way to study the effects of smoke exposure on patients, patient-to-patient variability is a major challenge for understanding of disease biogenesis and biomarker discovery, particularly for heterogeneous disorders like COPD. Therefore, there is a great need for a novel, versatile, and physiologically relevant experimental model that faithfully recapitulates inhaled smoke-induced airway pathologies to study the biological effects of tobacco products. An in vitro model of this type that reconstitutes clinically validated molecular, cellular and tissue-level responses of diseased human lung epithelium in an organ-relevant context would also have great value for discovery of potential therapeutic targets and new diagnostic biomarkers.

Most in vitro models used to study effects of smoking continuously expose cultured lung epithelial cells under static conditions to cigarette smoke extract (CSE) that primarily contains only its hydrophilic constituents (Glader et al., 2006; Mio et al., 1997; Mulligan et al., 2009) or to cigarette smoke condensate (CSC) composed of hydrophobic particulate matter (Hellermann et al., 2002). However, exposure to *whole* cigarette smoke, which contains particulate, hydrophobic, hydrophilic, and gaseous components, is required to induce the full complement of pathological phenotypes associated with smoke-induced airway injury (Adamson et al., 2011b; Thorne and Adamson, 2013). In studies with cultured lung cells, they are also often continuously exposed to CSE when submerged in liquid, rather

than being exposed at the air-liquid interface (ALI), which is known to be critical for normal lung airway biology (Pezzulo et al., 2011). A method for generating, diluting, and delivering whole cigarette smoke to lung epithelium cultured at an ALI was recently reported (Mathis et al., 2013; Phillips et al., 2005); however, this model only permits exposure of cells to vertically delivered puffs of smoke under *static* conditions. In contrast, human smokers commonly exhibit characteristic patterns of puff durations and volumes and inter-puff intervals that result in dynamic exposure to smoke compounds under conditions of flow that apply horizontal shear forces across the surface of the airway epithelium (Lee et al., 2003; Strasser et al., 2004).

Here, we describe an in vitro model of smoke-induced lung injury in which a microfluidic small airway-on-a-chip lined by living human bronchiolar epithelium cultured at an ALI (Benam et al., 2016) is connected to a smoking instrument that inhales and exhales whole smoke from burning cigarettes in and out of the epithelium-lined microchannel of the chip under dynamic conditions that faithfully recapitulate human smoking behavior. This platform was used to compare the effects of inhaled smoke on chips containing bronchiolar epithelium isolated from normal lungs or from lungs of COPD patients and to study the effects of e-cigarettes on human lung molecular, genetic, cellular, and tissue-level responses in vitro.

RESULTS

Engineering a Breathing Human Small Airway-on-a-Chip to Smoke Cigarettes

The smoking airway-on-a-chip consists of four integrated components: an organ-on-a-chip microfluidic device lined by human bronchiolar epithelium, a smoke generator, a microrespirator, and a control software that recapitulates human smoking behavior. The organ-on-a-chip is an optically clear, microfluidic culture device composed of poly(dimethylsiloxane) (PDMS) polymer the size of a computer memory stick that contains an upper microchannel (1 mm high × 1 mm wide) separated from a lower microchannel (0.2 mm high × 1 mm wide) by a thin, porous, polyester membrane (10 μm thick with 0.4 μm pores) coated with type I collagen (Figure 1A). Primary human airway epithelial cells (hAECs) obtained from healthy donors or COPD patients were cultured for 4 weeks on top of the membrane at an ALI while medium continuously flowed through the lower channel, as previously described (Benam et al., 2016). Under these conditions, the hAECs formed a highly differentiated pseudostratified ciliated airway epithelium and fully recapitulated the morphology and functions of the living lung small airway (Figures 1A and S1) (Benam et al., 2016).

To mimic exposure of the engineered human lung small airway to cigarette smoke on-chip, we constructed a microrespirator that cyclically breathes in and out microliter volumes of air through the upper epithelium-lined channel of the airway chip and a programmable smoke machine to regulate smoking behavioral parameters, such as puff duration and volume, inter-puff interval, puffs per cigarette, and the number of cigarettes smoked (Figures 1B, 1C, and S2; Movies S1 and S2). The channel geometry, air volume, and shear stress were scaled to reflect the expected values found in the generations 8–16 of airways in the lung. The entire apparatus was then placed in a standard culture incubator and connected with the chips and a peristaltic pump that controlled medium perfusion (Figure 1D). In the final assembly, the integrated microrespirator and smoking machine components worked in synchrony to flow freshly generated whole cigarette smoke horizontally across the surface of the differentiated epithelium only during the inhalation phase of the respiration cycle in the airway chip and to flow the smoke out during the exhalation phase.

Induction of Oxidative Stress in the Patient-Normalized Smoking Airway Chip

Cigarette smoke contains a complex combination of thousands of chemicals, some of which are oxidants and free radicals (Wooten et al., 2006), and this is reflected by higher oxidative stress levels in the lungs of smokers and COPD patients compared to healthy individuals (Comandini et al., 2010; Pierrou et al., 2007). To determine our ability to mimic acute smoke-induced airway injury responses and validate our system, we had the instrument sequentially "breathe" freshly produced whole cigarette smoke from nine research-grade 3R4F cigarettes into the upper, differentiated epithelium-lined channel of the chip over a period of 75 min and then analyzed responses the next day (Figures S3A and S3B). Analysis by phase-contrast microcopy showed homogeneous deposition of particulates over the entire length of the epithelium-lined channel (Figure S3C). When human airway chips fabricated using cells from normal (healthy) human donors were exposed to whole cigarette smoke using a smoking regimen (12 puffs per cigarette, 2 s puff duration, 22 s inter-puff intervals; sinusoidal respiratory flow of 150 μL air/smoke per breath, 12 breaths per minute) that is clinically relevant (Table 1), we consistently observed almost a 15-fold increase ($p < 0.01$) in expression of the antioxidant gene heme oxygenase 1 (HMOX1) compared to untreated controls when analyzed by qPCR (Figure 2A). Western blot analysis further revealed a significant ($p < 0.001$) increase in phosphorylation of the transcription factor nuclear factor (erythroid-derived 2)-like 2 (Nrf2) (Figures 2B and S4A), which has been shown to induce expression of cytoprotective genes, including HMOX1, to protect against oxidative stress and chemical toxicity (Ma, 2013).

To more comprehensively validate our model against human patient data, we performed genome-wide gene microarray analysis and compared our acute exposure results against those obtained by similar analysis of small airway epithelial cells isolated during bronchoscopy from phenotypically normal human smokers versus non-smokers using a published dataset (GEO: GSE4498) (Harvey et al., 2007). We identified 335 genes that exhibited significant changes ($p < 0.05$; fold change ≥ 2) in expression in normal smoking chips compared to non-smoking chips (Data S1), and a Gene Ontology functional enrichment analysis revealed 23 enriched biological processes (Figure 2C; Data S2). This analysis verified that oxidation-reduction pathway changes observed in human smokers are similarly modulated in our model. Moreover, closer examination of expression changes of genes associated with oxidation-reduction revealed striking similarities between human smokers and our smoking chips for a majority of genes (Figure 2D). The top three highly induced genes in all samples were aldo-keto reductase family 1 member B10 (AKR1B10), cytochrome P450 family 1 subfamily B polypeptide

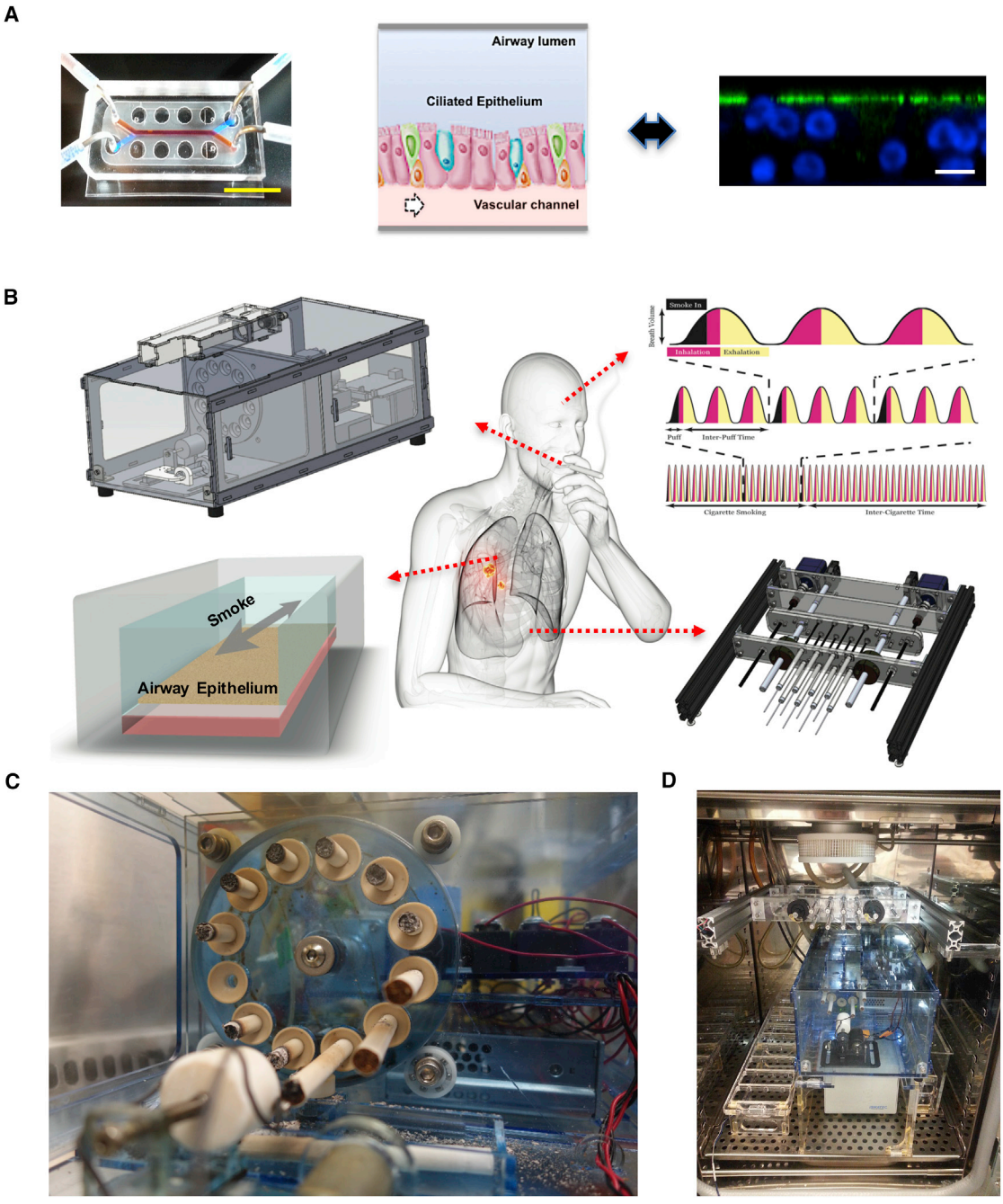

Figure 1. Testing Effects of Cigarette Smoke on Airway Epithelium In Vitro Using a Human Small Airway-on-a-Chip

(A) From left to right: a photograph of a small airway-on-a-chip microdevice (bar, 1 cm), a schematic diagram showing differentiated human mucociliated airway epithelium cultured in the top channel of the device, and a confocal fluorescence orthogonal micrograph showing cross-section of pseudostratified bronchiolar epithelium cultured on-chip for 4 weeks lined by apical cilia (green, β-tubulin IV; blue, DAPI-stained nuclei; bar, 10 μm).

(B) Schematic describing the overall method for analyzing effects of inhaled whole cigarette smoke in the lung small airway-on-a-chip. Cigarettes are loaded into a custom-engineered cigarette smoke machine (top left) that breathes smoke directly in and out of the lumen of the upper airway channel of the microchip (bottom left). Breathing and smoking topography parameters, including respiration cycle, puff time, and inter-puff interval, can be controlled as diagrammed schematically (top right) using the incubator shelf-compatible microrespirator component (bottom right). Smoking person image at center was acquired from Science Photo Library/SCIEPRO/Getty Images.

(C) Photos of the smoke machine component alone loaded with cigarettes (left) and the microrespirator and smoke machine combined setup located inside the incubator.

Table 1. Comparison of Smoking Parameters Used On-Chip versus in Human Smokers

Parameter	Clinical range	On-Chip
Puff duration	0.7–3 s	2 s
Inter-puff interval	17–26 s	22 s
Number of puffs per cigarette	8–14	12

Clinical values were obtained from published reports (Lee et al., 2003; Strasser et al., 2004).

1 (CYP1B1), and CYP1A1, and we independently confirmed this change in CYP1A1 expression by quantitative real-time PCR (Figure S4B). These findings are also consistent with past clinical studies, which showed that CYP1A1 is highly upregulated in airway epithelium of healthy smokers (Anttila et al., 2001).

Smoke-Induced Ciliary Dysfunction On-Chip

Smokers are often plagued by decreased mucociliary clearance; however, it is unclear whether this symptom is caused directly by ciliary dysfunction, because previous studies in humans and animal models have reported conflicting results, including increases, decreases, and no change in average ciliary beating frequencies (CBFs) in response to smoke exposure (Stanley et al., 1986; Yaghi et al., 2012; Zhou et al., 2009). Given the accessibility and visualization capabilities offered by the organ-on-chip method, we conducted an automated analysis of ciliary beat frequency in smoking versus untreated small airway chips using high-speed video microscopy to elucidate the effect of cigarette smoking on ciliary function. By using automated image processing to segment the images into regions with ciliary motion and then applying signal analysis to determine CBFs in the extracted regions (Figure S5), we were able to quantitatively map CBFs with single-cell resolution and at greater throughput than possible with traditional side view analysis of ciliary beating (Kim et al., 2011; Smith et al., 2012).

This analysis revealed that untreated small airway chips derived from multiple human donors faithfully recapitulated the normal Gaussian distribution of CBFs (Figures 3A and 3B) previously reported from analysis of nasal brushings or tissue (tracheal or bronchial) explants from healthy human donors cultured ex vivo (Olm et al., 2011; Wong et al., 1998). Airway chips exposed to cigarette smoke exhibited a comparable median CBF; however, the distribution of their CBFs was characterized by a 4-fold ($p < 0.05$) increase in variance (Figures 3C and 3D), as well as a negatively skewed shape of the distribution with a long tail extending into lower beat frequencies that no longer could be described by a normal distribution (Figure 3B). Intriguingly, this analysis revealed that smoking produces a heterogeneous effect on ciliary beating across the surface of the epithelium, with some areas beating normally and other beating at much reduced rates. Further, the skewed CBF distributions seen in smoke-exposed samples invalidate the use of statistics and associated tests of significance that assume a Gaussian distribution, such as the mean (average) value and the popular Student's t test. This may explain why past studies of human samples that only measured the effect of cigarette smoke on the average CBF produced conflicting results (Stanley et al., 1986; Yaghi et al., 2012; Zhou et al., 2009).

When compared the smoking airway chips with the same cells grown in transwell cultures, we found that this commonly used static culture model created artifacts that made it impossible to detect subtle changes in the distribution of CBFs. In particular, transwell models require that the differentiated epithelium be submerged in medium in order to be exposed to CSE. We found that this treatment alone increased the variance of CBFs by ~3-fold compared to cells maintained at the ALI, and subsequent exposure of these submerged cells to increasing concentrations (1%–4%) of CSE produced a decrease in variance of CBFs rather than the increase we observed on-chip in epithelium exposed to whole smoke under more physiological ALI conditions (Figure 3D). Our work further supports the recent shift away from CSE studies and toward approaches that rely upon ALI-mediated smoke exposure (Thorne and Adamson, 2013).

Airway Chip Platform to Study the Biological Effects of E-Cigarettes

To test the breadth and versatility of our platform, we explored whether the human small airway chip can be applied to study biological effects of e-cigarettes, specifically on oxidative stress and ciliary function. These studies revealed that when human small airway chips were exposed acutely to emissions from commercially available blu e-cigarettes under the same exposure regimen as the 3R4F tobacco cigarettes, there was no significant change in gene expression of HMOX1 (Figure 4A). Interestingly, while the ciliary beat distribution seemed to widen compared to controls, the change in the shape of the Gaussian distribution did not attain statistical significance (Figure 4B), and there also was no significant change in CBF variance (Figure 4C). Thus, our chip-based smoking platform can be used to discriminate differences in effects of conventional versus e-cigarettes on human lung epithelium.

Smoke-Induced Exacerbation of COPD On-Chip

Cigarette smoke is known to be a major non-infectious cause of clinical exacerbations in patients with COPD (Sapey and Stockley, 2006), and it cannot be modeled effectively in animals. We, therefore, set out to explore if we could mimic this relationship in human airway chips created with epithelial cells obtained from COPD patients, which have been previously shown to form a similarly well differentiated mucociliary epithelium after being maintained at ALI for 4 weeks on-chip (Benam et al., 2016), as this has never been examined previously in vitro. Clinical reports have demonstrated increased lung neutrophil accumulation and interleukin 8 (IL-8) levels in COPD patients who smoke compared with healthy subjects (Dickens et al., 2011; Keatings et al., 1996). When we stimulated airway chips with whole cigarette smoke, we observed that the COPD epithelium responded by producing large increases in secretion of IL-8, whereas there was no significant change in the healthy epithelium (Figure 5A).

We then compared gene expression profiles in COPD chips with or without smoke exposure using microarray analysis and identified 276 genes that were differentially expressed ($p < 0.05$; fold change ≥ 2) when COPD cells were exposed to cigarette smoke (Data S3), of which 147 were COPD specific and 129 were shared with smoke-exposed normal chips. We ranked the 147 COPD-unique genes based on their change in expression

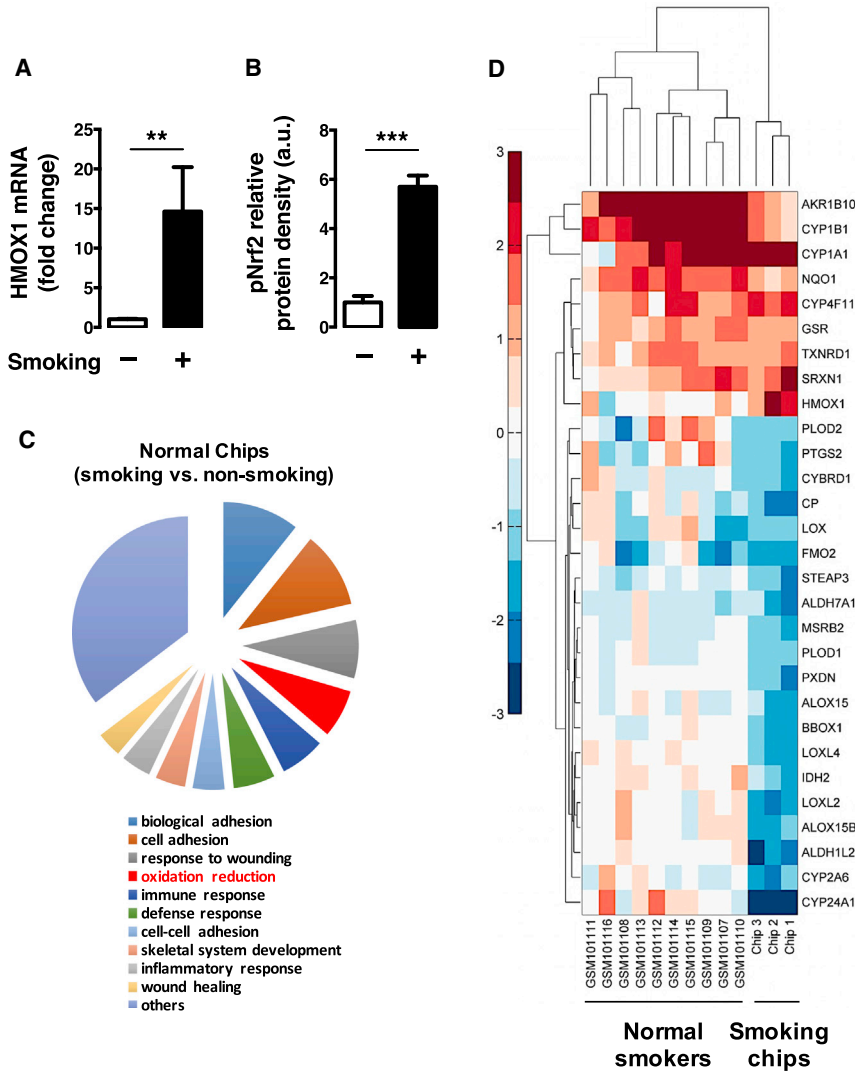

Figure 2. On-Chip Recapitulation of Smoke-Induced Oxidative Stress

(A) Real-time PCR analysis showed considerable upregulation of anti-oxidant heme oxygenase 1 (HMOX1) gene expression with smoke exposure (**$p < 0.01$; pooled data from three human donors with four biological replicates [chips] per donor; n = 12). Error bars indicate SEM.

(B) Graphic depiction of western blot analysis showing smoke-induced phosphorylation of the antioxidant regulator Nrf2 in epithelial cells on-chip (***$p < 0.001$; pooled data from two different normal human donors tested in three independent experiments (Figure S5A) with two biological replicates per donor; n = 4). Error bars indicate SEM.

(C) A pie chart showing the major biological processes with which genes that altered their expression in response to smoke exposure on-chip were associated, as determined using Gene Ontology analysis.

(D) A heatmap comparing expression of 29 genes associated with cellular oxidation-reduction in bronchiolar epithelial cells obtained by bronchoscopy-guided brushing of small airways from two different normal human smokers compared with samples obtained from three different human small airway chips that were exposed to whole cigarette smoke on-chip for 75 min. Note the general similarity in the patterns of both induced and suppressed genes. The color map indicates $\log_2$ fold changes in gene expression (upregulated genes in red, downregulated genes in blue).

relative to that observed in normal airway chips exposed to smoke (Data S4). This analysis revealed that the top ten genes represent a potentially novel set of genes that appear to distinguish differential responses to smoke exposure in COPD epithelium compared to healthy normal lung tissue (Figure 5B). These genes include metallothionein 1H (MT1H), transmembrane protease, serine 11E and 11F (TMPRSS11E and TMPRSS11F), matrix metallopeptidase 1 (MMP1), small proline rich protein 3 (SPRR3), repetin (RPTN), ATP6V0D2 (ATPase, H^+ transporting V0 subunit d2), ankyrin repeat domain 22 (ANKRD22), tetraspanin 7 (TSPAN7), and neuronal cell adhesion molecule (NRCAM). Importantly, changes in expression of these genes measured in normal airway epithelium on-chip were highly similar to those identified in human samples from normal donors (Figure 5B).

As clinical studies do not permit comparison of the effects of smoke exposure versus no exposure on the same individual, the variability among different patients within each population would be expected to be greater than that observed in the airway chips. Figure 5B highlights genes with significantly increased expression in response to acute smoke exposure in chips made with cells from COPD donors relative to chips not exposed to smoke and compares these expression levels to those measured in normal small airway chips exposed to smoke as well as to levels in normal (non-COPD) smokers in the clinical study. The fold change in mRNA levels for all of these genes did not surpass biological significance (>2-fold change) in either normal chips or the clinical samples (non-COPD smokers), whereas the COPD chips displayed a more than a 2-fold increase in all cases (Figure 5B).

One gene included in this list of key markers of the response of COPD epithelium to smoke exposure was MMP1, in line with published clinical reports on involvement of MMP-1 in COPD pathogenesis (Imai et al., 2001; Mercer et al., 2004). We validated smoke-induced MMP-1 upregulation at the protein level and, similar to IL-8, observed a hyperreactive response in COPD chips compared to normal chips (Figure S6A). Importantly, this effect was directly due to the combined effect of inhalation and whole smoke and not to breathing alone (Figure S6A). When we further analyzed relative expression of other metalloproteinase genes identified by the Gene Ontology analysis that differed in their expression between COPD and normal chips, we found that carboxypeptidase A4 (CPA4) and ADAM metallopeptidase with thrombospondin type 1 motif 1 (ADAMTS1) were also selectively induced in COPD cells (Figure S6B). To our knowledge, previous reports have not demonstrated the potential association of these genes with COPD and smoke-induced airway pathology.

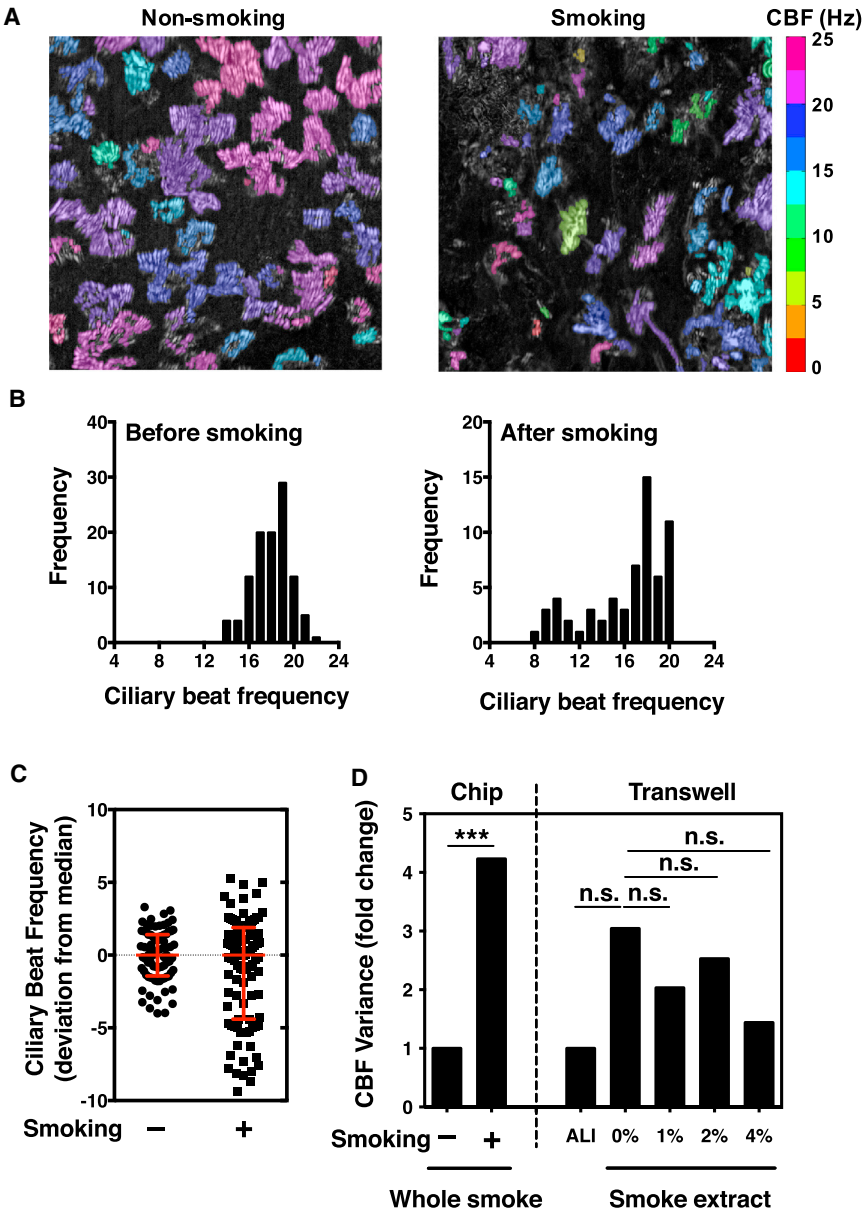

Figure 3. Physiological Recapitulation of Cigarette Smoke-Induced Ciliary Dysfunction On-Chip

(A) Representative time-lapse images of ciliary beating on the apical surface of the bronchiolar epithelium cultured on-chip in the absence (non-smoking) or presence (smoking) of whole cigarette smoke. Color table at right indicates ciliary beat frequency (CBF) of individual cilia. Note the increased range (variance) of beating frequencies in the smoke-exposed chips compared to control.

(B) Distributions of CBF in a representative normal small airway chip before and after smoking. Note that normal Gaussian distribution changes to a flattened, non-normal distribution after smoke exposure.

(C) Spread of ciliary beating frequencies (expressed as deviation from median CBF) measured in normal bronchiolar epithelium in the absence (–) or presence (+) of exposure to whole cigarette smoke on-chip for 24 hr. Data were pooled from two different human donors, with every symbol representing a measurement in one field of view [FOV] and more than 70 FOVs being analyzed for each condition; control tissue exhibited a Gaussian distribution of CBFs, whereas smoke-exposed tissue did not (non-smoking: FOV n = 80, chips n = 9, Shapiro-Wilk test, p = 0.1428; smoking: FOV n = 99; chips n = 9, Shapiro-Wilk test; p = 0.0002).

(D) A plot showing the fold change in variance of ciliary beating frequencies in normal airway epithelium cultured in the absence (–) or presence (+) of exposure to whole cigarette smoke on-chip (left) compared to similar results obtained with normal airway epithelium cultured in a transwell insert at an air-liquid interface before (ALI) and after (all results at right) being submerged in culture medium and exposed to 0%, 1%, 2%, or 4% cigarette smoke extract (CSE; Ansari-Bradley test, ***p < 0.001). n.s., not significant.

DISCUSSION

In this study, we described the development of an in vitro method for administrating whole smoke from tobacco or electronic cigarettes to differentiated normal or diseased human bronchiolar epithelium via inhaled and exhaled movements that mimic human smoking behavior. This method leverages a recently developed human small airway-on-a-chip model that recapitulates tissue- and organ-level structures and functions of the living human lung (Benam et al., 2016) and integrates it with a system composed of a smoke machine, microrespirator, and computer control system. The model provides a way to expose primary human airway cells from healthy normal donors and COPD patients matured into a differentiated airway epithelium at an ALI to physiological movements of air containing smoke from whole tobacco cigarettes or e-cigarettes using dynamic, clinically relevant smoking patterns in vitro and without empirical smoke dilutions. This smoking airway-on-a-chip culture system effectively recapitulated several key smoke-triggered molecular changes that are known to occur in lung epithelial cells, including increased oxidative stress (Comandini et al., 2010; Pierrou et al., 2007). Using the system with a highly sensitive automated imaging approach to evaluate smoke-related ciliopathies, we also gained insight into how smoke exposure alters ciliary motion in lung epithelium. Moreover, this system provided a reliable and versatile approach to study fine micropathologies, such as the pattern of ciliary beating. In addition, we reconstituted diseased tissue-specific responses in vitro and identified biomarkers in the form of a unique transcriptional signature that appears to distinguish responses to smoke exposure in COPD epithelium from those in healthy normal lung epithelium.

Smoke-induced oxidant damage to the lungs is a hallmark of airway pathology in COPD patients and smokers (Comandini et al., 2010; Pierrou et al., 2007). Our engineered smoking chips reproduced this cellular phenotype, as indicated by upregulated

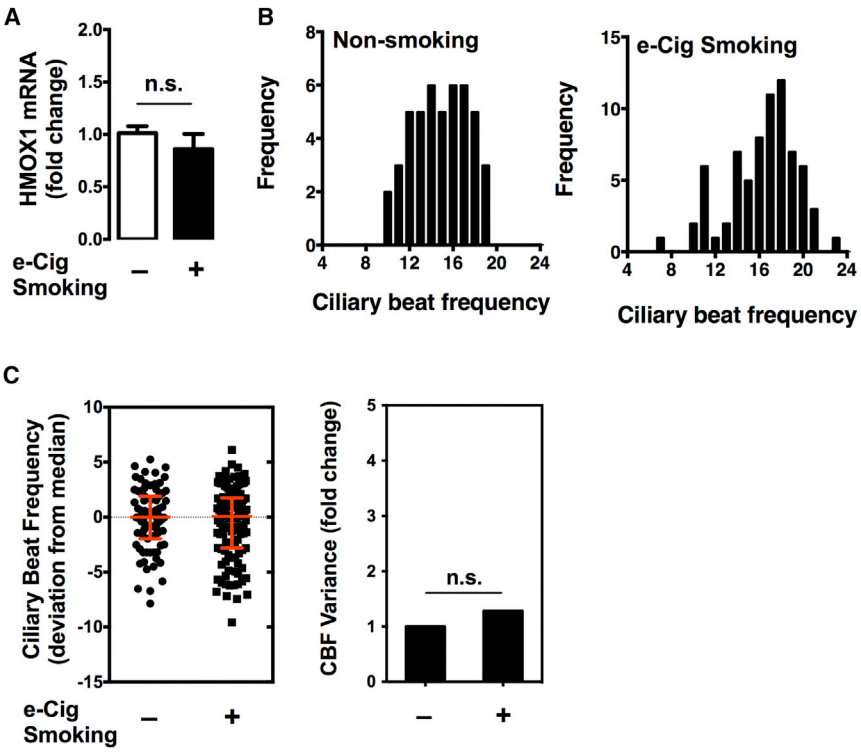

Figure 4. Testing Biological Effects of E-Cigarette Smoke Using the Small Airway-on-a-Chip

(A) Real-time PCR analysis did not detect a significant change in expression of (HMOX1) when normal lung epithelium was exposed on-chip to smoke generated from e-cigarettes generated and inhaled under the same regimen as 3R4F tobacco cigarettes, as shown in Figure 2 (pooled data from two human donors with three or four biological replicates per donor; n = 7–8). Error bars indicate SEM.

(B) CBF distributions in a representative normal small airway chip exposed to e-cigarette smoke (e-smoking) versus that observed in a non-smoking chip; both datasets follow a Gaussian distribution (non-smoking: FOV n = 79, chips n = 7, Shapiro-Wilk test, $p = 0.28$; e-smoking: FOV n = 119; chips n = 8, Shapiro-Wilk test; $p = 0.1$).

(C) A graph of the deviations from the median of CBF measured in normal bronchiolar epithelium in the absence (–) or presence (+) of exposure to e-cigarette smoke for 24 hr (left) and the fold-change in variance of the ciliary beating frequencies measured under these conditions (right), showing no significant difference (Ansari-Bradley test, $p = 0.1$).

HMOX1 gene expression and phosphorylated Nrf2. Notably, while a few published animal studies and CSE-treated in vitro models have shown similar results (Chen et al., 2010; Cipollina et al., 2014; Guan et al., 2013), none have performed comprehensive analysis of how the overall smoke-induced oxidative stress detected in their systems compare with clinical data. The whole-transcriptome analyses we carried out revealed that well-differentiated human airway epithelium challenged with whole cigarette smoke on-chip alters its expression of oxidation-reduction genes in a pattern that was similar to that previously observed in bronchoscopy samples (Harvey et al., 2007).

Interestingly, some of the COPD-specific genes identified in the airway chip studies (Figure 5B), such as MT1H, TMPRSS11E, TMPRSS11F, RPTN, and SPRR3, have not been associated with the COPD phenotype previously. MT1H, TMPRSS11E, and SPRR3 have been implicated in development of human malignancies (Gao et al., 2012; Han et al., 2013; Viloria et al., 2007) and potentially could explain at least in part why there is higher risk of lung cancer development in COPD smokers (Caramori et al., 2011). Moreover, selective upregulation of serine protease genes TMPRSS11E and TMPRSS11F may be in line with increased extracellular matrix degradation, airspace enlargement, and emphysema development in COPD lungs (Owen, 2008). Interestingly, TMPRSS11E has recently been reported to activate respiratory viruses such as influenza A viruses (Zmora et al., 2014); thus, our observation may in part explain higher susceptibility of COPD individuals to viral infections (Hsu et al., 2012). This can be studied by quantifying viral shedding and secretory inflammatory responses in COPD epithelia compared with healthy normal. In addition, induced expression of RPTN gene, which has been associated with epidermal and keratinocyte differentiation (Huber et al., 2005; Krieg et al., 1997), can potentially explain squamous metaplasia development observed in advanced stages of COPD pathogenesis (Puchelle et al., 2006). One potential approach to study this would be to expose the COPD chips to a range of whole cigarette smoke and compare secreted levels of repetin from the stimulated epithelia. Overall, our suggestions here are not meant to directly extrapolate the findings clinically; rather, we are highlighting the potential of our culture system over existing in vitro platforms for biomarker and therapeutic target discovery.

A key point in modeling complex and heterogeneous disorders like COPD is appreciating inter-individual differences. In fact, identification of 100% similarity in expression of *all* individual genes in a given patient population occurs at a very low frequency. Analysis of the bronchoscopy samples in Figure 2D revealed that some genes, such as LOX, were upregulated in some patients and downregulated in others. What is important here is that in the case of groups of genes, such as AKR1B10, CYP1B1, CYP1A1, NQO1, CYP2A6, FMO2, STEAP3, and others, which consistently exhibited similar trends in expression (i.e., they were either upregulated or downregulated in $\geq$80% of human bronchoscopy samples), the same trends were recapitulated using our smoking lung chip method. An even more crucial point here is that in contrast to human clinical studies, the human airway chips provide a major advantage by enabling a true matched comparison of biological responses as the cells lining the chips are sourced from the same patient donor and then cultured in the presence or absence of the same stimulus (in this case, smoke exposure), which normalizes for inter-individual variability. In addition, the chips support high-content analysis of airway epithelium from normal and COPD patients, which is not

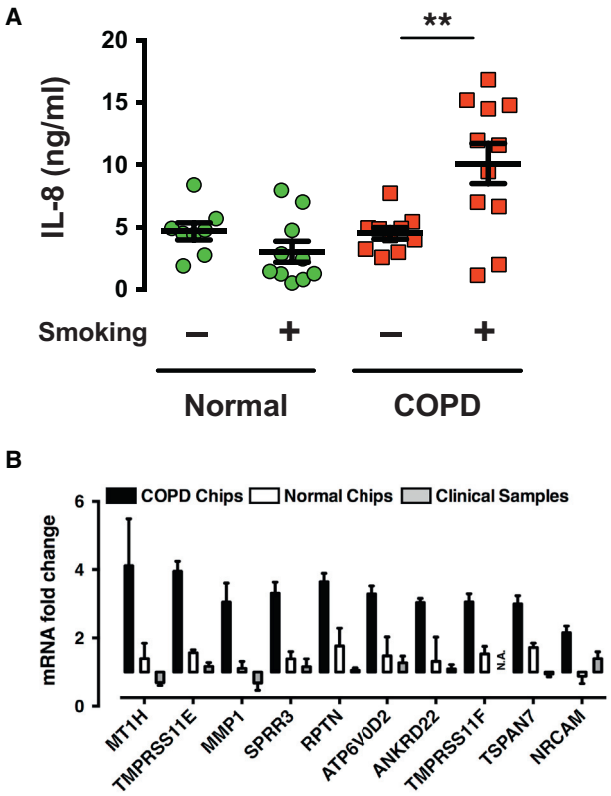

Figure 5. Modeling Smoke-Induced COPD Exacerbations On-Chip

(A) Quantitation of changes in secretion of interleukin 8 (IL-8) in small airway chips lined with bronchiolar epithelial cells isolated from normal or COPD patients with or without exposure to whole cigarette smoke for 75 min (smoking) (**$p < 0.01$; pooled data from five human donors, with two to five biological replicates per donor; n = 8–11). Error bars indicate SEM.

(B) Graph showing relative expression levels for the ten genes that were most significantly upregulated in COPD chips (black bars) or normal chips (white bars) after smoke exposure for 75 min compared with induction of expression levels of the same genes in bronchoscopy samples of bronchiolar epithelial cells from normal human smokers relative to non-smokers (gray bars). Note the close match between results obtained with the chips and the clinical donor samples: metallothionein 1H (MT1H), transmembrane protease, serine 11E (TMPRSS11E), small proline rich protein 3 (SPRR3), repetin (RPTN), ATP6V0D2 (ATPase, H^+ transporting V0 subunit d2), ankyrin repeat domain 22 (ANKRD22), transmembrane protease, serine 11F (TMPRSS11F), tetraspanin 7 (TSPAN7), neuronal cell adhesion molecule (NRCAM). Error bars indicate SD. N.A., no transcriptomic clinical data was available.

possible or extremely difficult to perform in conventional human clinical bronchoscopy studies. Thus, using the chips it may be possible to identify subtle yet potentially clinically relevant gene expression changes that would have been otherwise missed in studies involving individuals with COPD or other heterogeneous patient populations. Finally, while most clinical studies investigate human subjects with several years of smoking history (Pierrou et al., 2007), we discovered that acute intense exposure to smoke in our chips induces a similar phenotype to that observed in the chronic smokers. Thus, given the high similarity in expression of most oxidation-reduction genes between clinical and chip samples, the chip technology may offer a simpler and more rapid way to recreate these pathological phenotypes, in addition to enabling study of the molecular mechanisms that underlie this response in vitro.

Another major advantage of the smoking chip method over widely used existing culture models is that our system permits exposure to whole cigarette smoke (as opposed to CSE or CSC) under physiologically relevant breathing conditions without disrupting the ALI. This is important, because we found that submersion of the epithelium under fluid medium was alone sufficient to alter CBF variability. Additionally, using an automated method for evaluating CBF, we discovered two changes in ciliary function induced by smoke exposure: enhanced beat frequency variability and transformation of the normal Gaussian ciliary beating distribution to a non-normal pattern. This method offers an improved analytical approach to explain reduced mucociliary clearance observed in smokers' lungs (Vastag et al., 1986). Thus, two technological advances that our platform offers compared to alternative in vitro models are development of a programmable experimental system that can apply whole cigarette smoke to well-differentiated primary human lung airway epithelium and a method for quantification of the effects of smoke on ciliary beat frequency. Moreover, our engineered system provided a way to discriminate between effects of smoke produced by whole cigarettes versus e-cigarettes, with the latter only altering the beating distribution.

It is not possible to perform accurate side-by-side comparison of chip technology against current in vitro whole-smoke exposure systems, such as the Vitrocell model (Mathis et al., 2013; Neilson et al., 2015), as our system utilizes observed smoke behavior as input parameters and produces a dynamic smoke-air pattern in the tissue under physiologically relevant shear stress compared to empirically diluted smoke that is presented under static conditions in the commercial systems. Importantly, the commercial systems have primarily been used to study cytotoxicity and, to our knowledge, have never been used to recreate diseased tissue-specific responses or for discovery of biomarkers.

The use of e-cigarettes is on the rise; however, regulation by the Food and Drug Administration (FDA), as well as our understanding of e-cigarettes' impact on health, have not been able to keep up with the rapid pace of their use (Rowell and Tarran, 2015). A few studies have addressed toxicity of e-cigarette aerosols or e-liquids in vitro (Cervellati et al., 2014; Misra et al., 2014; Neilson et al., 2015; Shivalingappa et al., 2015); however, they neither recreated physiological breathing movements during exposure nor identified subtle micropathologies, such as transformation of CBF distributions, as we did using the chip technology.

One limitation of our system is the absence of other lung parenchymal cells, such as fibroblasts. Indeed, given the significant upregulation of MMP-1 release as well as induced TMPRSS11E gene expression from COPD epithelia on-chip, it would be interesting to study how this may impact extracellular matrix homeostasis and fibroblast function locally. Integration of pulmonary fibroblasts and/or airway smooth muscle cells might not only drive a fibrotic response but also enhance the local oxidative stress response in epithelium via secretion of hydrogen peroxide (Sakai and Tager, 2013). Moreover, we have previously shown that co-culture of airway epithelium with lung microvascular endothelial cells in the chip can

augment secretion of several pro-inflammatory cytokines and chemokines into the vascular channel (Benam et al., 2016). Thus, inclusion of the endothelium might lead to an exaggerated response to exposure to cigarette smoke, and if immune cells were flowed through the vascular channel, they might be stimulated to bind to the endothelium and further support this cytokine cascade. Additionally, to more thoroughly investigate the cytotoxic effects of e-cigarettes, a long-term exposure model lasting several days to a few weeks would be more appropriate.

It is important to note that the smoking airway chip technology is a synthetic system that allows study of potential cellular and molecular contributors to organ-level pathophysiology, as well as interrogation of different assumptions in the field, such as the absolute requirement for circulating immune cells to recapitulate a particular organ-level response. Using this synthetic biology approach, we started with the simplest model and explored whether it can or cannot mimic organ-level physiology or pathophysiology. In our past published work, we specifically were exploring the effects of inhibitors of inflammation on recruitment of circulating immune cells, and thus, we could not mimic the relevant biology without including both endothelium and immune cells (Benam et al., 2016). In contrast, in the present study, we started with the simplest embodiment of the model first (using only differentiated airway epithelium in one microchannel while flowing medium through the second channel without an endothelium) and found that we could mimic many of the organ-level pathologies and human tissue sensitivities exhibited by human patients with COPD compared to healthy cells. This finding alone (that other cell types beyond the differentiated epithelium are not required to manifest these varied effects of smoke inhalation) is important and could not be accomplished using a mouse model or other culture models that do not permit delivery of inhaled air containing whole smoke under ''active,'' physiological breathing conditions.

In conclusion, the smoking human small airway chip method provides a tool for studying airway pathophysiology at multiple system levels and enables true matched comparisons of biological responses to inhaled smoke generated by either whole cigarettes or e-cigarettes. It also can be used to identify COPD-specific biological responses and discover novel molecular signatures that may serve as potential therapeutic targets or diagnostic biomarkers.

STAR★METHODS

Detailed methods are provided in the online version of this paper and include the following:

SUPPLEMENTAL INFORMATION

Supplemental Information includes six figures, one table, two movies, and four datasets and can be found with this article online at http://dx.doi.org/10.1016/j.cels.2016.10.003.

AUTHOR CONTRIBUTIONS

K.H.B., R.N., and D.E.I. designed the research; K.H.B., R.N., and Y.C. designed the smoking machine; R.N. and Y.C. fabricated the smoking machine; T.C.F. fabricated the chip microrespirator; K.H.B prepared, cultured, and smoked airway chips; M.H.K. performed western blotting analysis; K.H.B. performed immunostaining for confocal imaging and qPCR; J.C.W. performed SEM imaging; K.H.B. and J.N. recorded and analyzed CBF data; K.H.B. and R.N. analyzed the microarray data; R.N. and J.N. performed statistical analyses; K.H.B., R.N., and J.N. prepared the manuscript; R.P.B., K.K.P., and A.B. commented on the manuscript; and D.E.I. critically revised the manuscript.

ACKNOWLEDGMENTS

We thank J. Sliz for help with the initial microrespirator design, the Wyss Institute Microfabrication Team for chip fabrication, B. Boettner for assistance with manuscript preparation, and S.A. Kroll and A. Giampaolo for assistance with video acquisition. This work was supported by the Wyss Institute for Biologically Inspired Engineering at Harvard University and Defense Advanced Research Projects Agency (DARPA) under cooperative agreement number W911NF-12-2-0036. D.E.I. holds equity in Emulate, Inc. and Opsonix, Inc. and chairs their scientific advisory boards. D.E.I., K.H.B., R.N., T.C.F., and Y.C. are inventors on one provisional patent application that covers the breathing-smoking lung chip technology, and D.E.I., K.H.B., and R.N. are inventors on another provisional patent application that describes novel therapeutic-diagnostic biomarkers in COPD.

Received: May 21, 2016
Revised: August 15, 2016
Accepted: October 5, 2016
Published: October 27, 2016

REFERENCES

Adamson, J., Haswell, L.E., Phillips, G., and Gaça, M.D. (2011a). In vitro models of chronic obstructive pulmonary disease (COPD). In Bronchitis, I. MartÃn-Loeches, ed. (InTech), pp. 41–66.

Adamson, J., Azzopardi, D., Errington, G., Dickens, C., McAughey, J., and Gaça, M.D. (2011b). Assessment of an in vitro whole cigarette smoke exposure system: The Borgwaldt RM20S 8-syringe smoking machine. Chem. Cent. J. *5*, 50.

Anttila, S., Tuominen, P., Hirvonen, A., Nurminen, M., Karjalainen, A., Hankinson, O., and Elovaara, E. (2001). CYP1A1 levels in lung tissue of tobacco smokers and polymorphisms of CYP1A1 and aromatic hydrocarbon receptor. Pharmacogenetics *11*, 501–509.

Benam, K.H., Kok, W.L., McMichael, A.J., and Ho, L.P. (2011). Alternative spliced CD1d transcripts in human bronchial epithelial cells. PLoS ONE *6*, e22726.

Benam, K.H., Villenave, R., Lucchesi, C., Varone, A., Hubeau, C., Lee, H.H., Alves, S.E., Salmon, M., Ferrante, T.C., Weaver, J.C., et al. (2016). Small airway-on-a-chip enables analysis of human lung inflammation and drug responses in vitro. Nat. Methods *13*, 151–157.

Caramori, G., Adcock, I.M., Casolari, P., Ito, K., Jazrawi, E., Tsaprouni, L., Villetti, G., Civelli, M., Carnini, C., Chung, K.F., et al. (2011). Unbalanced oxidant-induced DNA damage and repair in COPD: a link towards lung cancer. Thorax *66*, 521–527.

Cervellati, F., Muresan, X.M., Sticozzi, C., Gambari, R., Montagner, G., Forman, H.J., Torricelli, C., Maioli, E., and Valacchi, G. (2014). Comparative effects between electronic and cigarette smoke in human keratinocytes and epithelial lung cells. Toxicology In Vitro *28*, 999–1005.

Chen, H., Wang, L., Gong, T., Yu, Y., Zhu, C., Li, F., Wang, L., and Li, C. (2010). EGR-1 regulates Ho-1 expression induced by cigarette smoke. Biochem. Biophys. Res. Commun. *396*, 388–393.

Cipollina, C., Di Vincenzo, S., Gerbino, S., Siena, L., Gjomarkaj, M., and Pace, E. (2014). Dual anti-oxidant and anti-inflammatory actions of the electrophilic cyclooxygenase-2-derived 17-oxo-DHA in lipopolysaccharide- and cigarette smoke-induced inflammation. Biochim. Biophys. Acta *1840*, 2299–2309.

Comandini, A., Marzano, V., Curradi, G., Federici, G., Urbani, A., and Saltini, C. (2010). Markers of anti-oxidant response in tobacco smoke exposed subjects: a data-mining review. Pulm. Pharmacol. Ther. *23*, 482–492.

Dickens, J.A., Miller, B.E., Edwards, L.D., Silverman, E.K., Lomas, D.A., and Tal-Singer, R.; Evaluation of COPD Longitudinally to Identify Surrogate Endpoints (ECLIPSE) study investigators (2011). COPD association and repeatability of blood biomarkers in the ECLIPSE cohort. Respir. Res. *12*, 146.

Gao, H., Wang, L., Cui, S., and Wang, M. (2012). Combination of meta-analysis and graph clustering to identify prognostic markers of ESCC. Genet. Mol. Biol. *35*, 530–537.

Glader, P., Möller, S., Lilja, J., Wieslander, E., Löfdahl, C.G., and von Wachenfeldt, K. (2006). Cigarette smoke extract modulates respiratory defence mechanisms through effects on T-cells and airway epithelial cells. Respir. Med. *100*, 818–827.

Guan, S.P., Tee, W., Ng, D.S., Chan, T.K., Peh, H.Y., Ho, W.E., Cheng, C., Mak, J.C., and Wong, W.S. (2013). Andrographolide protects against cigarette smoke-induced oxidative lung injury via augmentation of Nrf2 activity. Br. J. Pharmacol. *168*, 1707–1718.

Han, Y.C., Zheng, Z.L., Zuo, Z.H., Yu, Y.P., Chen, R., Tseng, G.C., Nelson, J.B., and Luo, J.H. (2013). Metallothionein 1 h tumour suppressor activity in prostate cancer is mediated by euchromatin methyltransferase 1. J. Pathol. *230*, 184–193.

Harvey, B.G., Heguy, A., Leopold, P.L., Carolan, B.J., Ferris, B., and Crystal, R.G. (2007). Modification of gene expression of the small airway epithelium in response to cigarette smoking. J. Mol. Med. *85*, 39–53.

Hellermann, G.R., Nagy, S.B., Kong, X., Lockey, R.F., and Mohapatra, S.S. (2002). Mechanism of cigarette smoke condensate-induced acute inflammatory response in human bronchial epithelial cells. Respir. Res. *3*, 22.

Hogg, J.C., McDonough, J.E., and Suzuki, M. (2013). Small airway obstruction in COPD: new insights based on micro-CT imaging and MRI imaging. Chest *143*, 1436–1443.

Hsu, A.C., See, H.V., Hansbro, P.M., and Wark, P.A. (2012). Innate immunity to influenza in chronic airways diseases. Respirology *17*, 1166–1175.

Huang da, W., Sherman, B.T., and Lempicki, R.A. (2009). Systematic and integrative analysis of large gene lists using DAVID bioinformatics resources. Nat. Protoc. *4*, 44–57.

Huber, M., Siegenthaler, G., Mirancea, N., Marenholz, I., Nizetic, D., Breitkreutz, D., Mischke, D., and Hohl, D. (2005). Isolation and characterization of human repetin, a member of the fused gene family of the epidermal differentiation complex. J. Invest. Dermatol. *124*, 998–1007.

Imai, K., Dalal, S.S., Chen, E.S., Downey, R., Schulman, L.L., Ginsburg, M., and D'Armiento, J. (2001). Human collagenase (matrix metalloproteinase-1) expression in the lungs of patients with emphysema. Am. J. Respir. Crit. Care Med. *163*, 786–791.

Keatings, V.M., Collins, P.D., Scott, D.M., and Barnes, P.J. (1996). Differences in interleukin-8 and tumor necrosis factor-alpha in induced sputum from patients with chronic obstructive pulmonary disease or asthma. Am. J. Respir. Crit. Care Med. *153*, 530–534.

Kim, W., Han, T.H., Kim, H.J., Park, M.Y., Kim, K.S., and Park, R.W. (2011). An automated measurement of ciliary beating frequency using a combined optical flow and peak detection. Healthc. Inform. Res. *17*, 111–119.

Krieg, P., Schuppler, M., Koesters, R., Mincheva, A., Lichter, P., and Marks, F. (1997). Repetin (Rptn), a new member of the "fused gene" subgroup within the S100 gene family encoding a murine epidermal differentiation protein. Genomics *43*, 339–348.

Lee, E.M., Malson, J.L., Waters, A.J., Moolchan, E.T., and Pickworth, W.B. (2003). Smoking topography: reliability and validity in dependent smokers. Nicotine Tob. Res. *5*, 673–679.

Ma, Q. (2013). Role of nrf2 in oxidative stress and toxicity. Annu. Rev. Pharmacol. Toxicol. *53*, 401–426.

Mathis, C., Poussin, C., Weisensee, D., Gebel, S., Hengstermann, A., Sewer, A., Belcastro, V., Xiang, Y., Ansari, S., Wagner, S., et al. (2013). Human bronchial epithelial cells exposed in vitro to cigarette smoke at the air-liquid interface resemble bronchial epithelium from human smokers. Am. J. Physiol. Lung Cell. Mol. Physiol. *304*, L489–L503.

Mercer, B.A., Kolesnikova, N., Sonett, J., and D'Armiento, J. (2004). Extracellular regulated kinase/mitogen activated protein kinase is up-regulated in pulmonary emphysema and mediates matrix metalloproteinase-1 induction by cigarette smoke. J. Biol. Chem. *279*, 17690–17696.

Mio, T., Romberger, D.J., Thompson, A.B., Robbins, R.A., Heires, A., and Rennard, S.I. (1997). Cigarette smoke induces interleukin-8 release from human bronchial epithelial cells. Am. J. Respir. Crit. Care Med. *155*, 1770–1776.

Misra, M., Leverette, R.D., Cooper, B.T., Bennett, M.B., and Brown, S.E. (2014). Comparative in vitro toxicity profile of electronic and tobacco cigarettes, smokeless tobacco and nicotine replacement therapy products: e-liquids, extracts and collected aerosols. Int. J. Environ. Res. Public Health *11*, 11325–11347.

Mulligan, R.M., Atkinson, C., Vertegel, A.A., Reukov, V., and Schlosser, R.J. (2009). Cigarette smoke extract stimulates interleukin-8 production in human airway epithelium and is attenuated by superoxide dismutase in vitro. Am. J. Rhinol. Allergy *23*, e1–e4.

Neilson, L., Mankus, C., Thorne, D., Jackson, G., DeBay, J., and Meredith, C. (2015). Development of an in vitro cytotoxicity model for aerosol exposure using 3D reconstructed human airway tissue; application for assessment of e-cigarette aerosol. Toxicology In Vitro *29*, 1952–1962.

Olm, M.A., Kogler, J.E., Jr., Macchione, M., Shoemark, A., Saldiva, P.H., and Rodrigues, J.C. (2011). Primary ciliary dyskinesia: evaluation using cilia beat frequency assessment via spectral analysis of digital microscopy images. J. Appl. Physiol. *111* (1985), 295–302.

Owen, C.A. (2008). Roles for proteinases in the pathogenesis of chronic obstructive pulmonary disease. Int. J. Chron. Obstruct. Pulmon. Dis. *3*, 253–268.

Pezzulo, A.A., Starner, T.D., Scheetz, T.E., Traver, G.L., Tilley, A.E., Harvey, B.G., Crystal, R.G., McCray, P.B., Jr., and Zabner, J. (2011). The air-liquid interface and use of primary cell cultures are important to recapitulate the transcriptional profile of in vivo airway epithelia. Am. J. Physiol. Lung Cell. Mol. Physiol. *300*, L25–L31.

Phillips, J., Kluss, B., Richter, A., and Massey, E. (2005). Exposure of bronchial epithelial cells to whole cigarette smoke: assessment of cellular responses. Altern. Lab. Anim. *33*, 239–248.

Pierrou, S., Broberg, P., O'Donnell, R.A., Pawłowski, K., Virtala, R., Lindqvist, E., Richter, A., Wilson, S.J., Angco, G., Möller, S., et al. (2007). Expression of genes involved in oxidative stress responses in airway epithelial cells of smokers with chronic obstructive pulmonary disease. Am. J. Respir. Crit. Care Med. *175*, 577–586.

Powell, H.A., Iyen-Omofoman, B., Baldwin, D.R., Hubbard, R.B., and Tata, L.J. (2013). Chronic obstructive pulmonary disease and risk of lung cancer: the importance of smoking and timing of diagnosis. J. Thoracic Oncol. *8*, e34–e35.

Puchelle, E., Zahm, J.M., Tournier, J.M., and Coraux, C. (2006). Airway epithelial repair, regeneration, and remodeling after injury in chronic obstructive pulmonary disease. Proc. Am. Thorac. Soc. *3*, 726–733.

Rennard, S.I., and Drummond, M.B. (2015). Early chronic obstructive pulmonary disease: definition, assessment, and prevention. Lancet *385*, 1778–1788.

Rowell, T.R., and Tarran, R. (2015). Will chronic e-cigarette use cause lung disease? Am. J. Physiol. Lung Cell. Mol. Physiol. *309*, L1398–L1409.

Sakai, N., and Tager, A.M. (2013). Fibrosis of two: epithelial cell-fibroblast interactions in pulmonary fibrosis. Biochim. Biophys. Acta *1832*, 911–921.

Sapey, E., and Stockley, R.A. (2006). COPD exacerbations. 2: aetiology. Thorax *61*, 250–258.

Shivalingappa, P.C., Hole, R., Westphal, C.V., and Vij, N. (2015). Airway exposure to e-cigarette vapors impairs autophagy and induces aggresome formation. Antioxid. Redox Signal. Published online October 27, 2015. http://dx.doi.org/10.1089/ars.2015.6367.

Smith, C.M., Djakow, J., Free, R.C., Djakow, P., Lonnen, R., Williams, G., Pohunek, P., Hirst, R.A., Easton, A.J., Andrew, P.W., and O'Callaghan, C. (2012). ciliaFA: a research tool for automated, high-throughput measurement of ciliary beat frequency using freely available software. Cilia *1*, 14.

Stanley, P.J., Wilson, R., Greenstone, M.A., MacWilliam, L., and Cole, P.J. (1986). Effect of cigarette smoking on nasal mucociliary clearance and ciliary beat frequency. Thorax *41*, 519–523.

Strasser, A.A., Pickworth, W.B., Patterson, F., and Lerman, C. (2004). Smoking topography predicts abstinence following treatment with nicotine replacement therapy. Cancer Epidemiol. Biomarkers Prev. *13*, 1800–1804.

Thorne, D., and Adamson, J. (2013). A review of in vitro cigarette smoke exposure systems. Exp. Toxicol. Pathol. *65*, 1183–1193.

Vastag, E., Matthys, H., Zsamboki, G., Köhler, D., and Daikeler, G. (1986). Mucociliary clearance in smokers. Eur. J. Respir. Dis. *68*, 107–113.

Viloria, C.G., Peinado, J.R., Astudillo, A., García-Suárez, O., González, M.V., Suárez, C., and Cal, S. (2007). Human DESC1 serine protease confers tumorigenic properties to MDCK cells and it is upregulated in tumours of different origin. Br. J. Cancer *97*, 201–209.

Vlahos, R., and Bozinovski, S. (2014). Recent advances in pre-clinical mouse models of COPD. Clin. Sci. *126*, 253–265.

Wong, L.B., Park, C.L., and Yeates, D.B. (1998). Neuropeptide Y inhibits ciliary beat frequency in human ciliated cells via nPKC, independently of PKA. Am. J. Physiol. *275*, C440–C448.

Wooten, J.B., Chouchane, S., and McGrath, T.E. (2006). Tobacco smoke constituents affecting oxidative stress. In Cigarette Smoke and Oxidative Stress, B.B. Halliwell and H.E. Poulsen, eds. (Springer), p. 407.

Wright, J.L., Cosio, M., and Churg, A. (2008). Animal models of chronic obstructive pulmonary disease. Am. J. Physiol. Lung Cell. Mol. Physiol. *295*, L1–L15.

Yaghi, A., Zaman, A., Cox, G., and Dolovich, M.B. (2012). Ciliary beating is depressed in nasal cilia from chronic obstructive pulmonary disease subjects. Respir. Med. *106*, 1139–1147.

Zhou, H., Wang, X., Brighton, L., Hazucha, M., Jaspers, I., and Carson, J.L. (2009). Increased nasal epithelial ciliary beat frequency associated with lifestyle tobacco smoke exposure. Inhal. Toxicol. *21*, 875–881.

Zmora, P., Blazejewska, P., Moldenhauer, A.S., Welsch, K., Nehlmeier, I., Wu, Q., Schneider, H., Pöhlmann, S., and Bertram, S. (2014). DESC1 and MSPL activate influenza A viruses and emerging coronaviruses for host cell entry. J. Virol. *88*, 12087–12097.

STAR★METHODS

KEY RESOURCES TABLE

REAGENT or RESOURCE	SOURCE	IDENTIFIER
Antibodies		
Rabbit anti-Nrf2 (phosphor S40) antibody	Abcam	Cat.# ab76026
Rabbit anti-Nrf2 antibody	Abcam	Cat.# ab62352
Mouse anti-GAPDH antibody	Millipore	Cat.# AB2302
Critical Commercial Assays		
Human Cytokine/Chemokine (for IL-8) and MMP (for MMP-1) Magnetic Bead Panel	Millipore	Cat.# HCYTOMAG-60K, and HMMP2MAG-55K
Deposited Data		
Raw and analyzed data	This paper	GEO: GSE87098
Clinical bronchoscopy (smoking and non-smoking) bronchiolar samples raw microarray data	Harvey et al., 2007	GEO: GSE4498
Sequence-Based Reagents		
Primer for CYP1A1 Forward: ACCTACCCAACCCTTCCCTGA	This paper	N/A
Primer for CYP1A1 Reverse: AGGCTGTCTGTGATGTCCCG	This paper	N/A
Primer for HMOX1 Forward: ACTTTCAGAAGGGCCAGGTG	This paper	N/A
Primer for HMOX1 Reverse: GACTGGGCTCTCCTTGTTGC	This paper	N/A
Primer for HPRT Forward: GACTTTGCTTTCCTTGGTCAGG	Benam et al., 2011	N/A
Primer for HPRT Reverse: AGTCTGGCTTATATCCAACACTTCG	Benam et al., 2011	N/A
Software and Algorithms		
Microrespirator and smoking instrument software	This paper	N/A
Ciliary beat frequency data analysis	This paper	N/A
Database for Annotation, Visualization and Integrated Discovery (DAVID)	Huang da et al., 2009	https://david.ncifcrf.gov
Other		
Small Airway Epithelial Cell Basal Medium	Promocell	Cat.# C-21270
Small Airway Epithelial Cell Growth Medium SupplementPack	Promocell	Cat.# C-39170
Biochip-compatible smoking instrument	This paper	N/A
Microrespirator	This paper	N/A
3R4F Reference Cigarettes	University of Kentucky, Center for Tobacco Reference Products	3R4F Cigarettes
blu Classic Tobacco-Flavor Disposable Electronic Cigarette	7 Eleven	N/A
Polyester Membrane Transwell-Clear Inserts with 0.4 μm Pores	Corning	Cat.# 3470

CONTACT FOR REAGENT AND RESOURCE SHARING

As Lead Contact, Don Ingber is responsible for all reagents and resource requests. Please contact Don Ingber at don.ingber@wyss.harvard.edu with requests and inquiries.

EXPERIMENTAL MODEL AND SUBJECT DETAILS

Primary human small airway epithelial cells were purchased from Promocell (Germany), Epithelix (Switzerland) and Lonza (USA).

METHOD DETAILS

Microfluidic Chip Fabrication

Molds for the microfluidic devices were fabricated out of Prototherm 12120 using stereolithography (Protolabs, Maple Plain, MN). The top and bottom components of the devices were cast from polydimethyl siloxane (PDMS) at a 10:1 w/w base to curing agent ratio, degassed, and cured for 4 hr to overnight at 60°C. The top component contains a fluidic channel (1 × 1 mm cross section) and ports

for the top and bottom channels. This is bonded, using oxygen plasma treatment (40 W, 800 mbar, 40 s; Plasma Nano, Diener Electronic, Ebhausen, Germany), to the bottom component containing the endothelial channel (1 mm wide x 0.2 mm high). A laser cut 0.4 μm pore diameter track-etched PET membrane (~10 μm thick; Maine Manufacturing, Sanford, ME) is sandwiched between the components to provide a semi-permeable barrier between the airway epithelium and microvascular endothelium layers. Devices were sterilized using oxygen plasma treatment (100 W, 15 sccm, 30 s; PlasmaEtcher PE-100, Plasma Etch, Reno, NV).

Microfluidic Organ-on-a-Chip Cell Culture

Primary human small airway epithelial cells were expanded in 75 cm^2 tissue culture flasks using small airway epithelial growth medium supplemented with growth factors (Promocell) until ~80% confluent. Detailed methods for culture and differentiation of human lung epithelial cells in airway chip have been recently described (Benam et al., 2016). Briefly, bronchiolar cells were seeded onto the membrane, maintained in a submerged state for 5 days and an air-liquid interface was established in the upper channel for 3 to 5 weeks, while the bottom channel was perfused with medium. Chips were then transferred to designated incubator for smoke exposure.

Design of Biochip-Compatible Breathing-Smoking Instrument

The smoking instrument was designed to accommodate up to 10 cigarettes of various brands and mimic the range of typical smoker behaviors. Briefly, the instrument holds up to 10 cigarettes in a revolving holder with airtight silicone sealing rings. The control software triggers the ignition of each cigarette using a solenoid-actuated nichrome wire coil mounted on a ceramic mount inside a Teflon conical adaptor. A miniature vacuum pump provides air intake during ignition and during each "puff" and draws air from the cigarette, through a Teflon mouthpiece, to a 5 mL smoke reservoir. This action occurs at arbitrary user-selectable intervals (Figure S3). A first pinch valve is used to programmatically select the timing of smoke and incubator air entering the chips during each inhalation. A second pinch valve directs the flow of air, routing smoke or air into the chips during inhalation and out of the chips into the exhaust during exhalation. An onboard microcontroller, relays, and a power supply provide support and communication with an external laptop. The system is controlled by custom LabView software that enables users to define a broad range of smoker behavior parameters; however, we used a clinically relevant range in the present study (Table 1).

Microrespirator Design and Operation

The microrespirator consists of 8 air-tight 500 μL glass syringes cyclically actuated using a stepper motor-driven leadscrew and mounted in an aluminum and acrylic frame. The Arduino control software provides configurable sinusoidal respiratory flow of 150 μL in 2.5 s inhalation and 2.5 s exhalation times and is monitored by the smoking instrument. This air volume was calculated to meet our goal of modeling bronchiole generations 8-16, which are on average approximately 1 mm in diameter. Using measurements of human lung total cross sectional areas at these bifurcations (25-50 cm^2) (Hogg et al., 2013) and a typical breath volume of 0.5 l at 5 s cycle times, we calculated an approximate air volume of 150 μL per inhalation would be required to model in vivo conditions for our 0.01 cm^2 epithelial channel cross sectional area.

Exposure of Small Airway Epithelium to Flowing Whole Cigarette Smoke on-Chip

One outlet of 'airway lumen' channel of well-differentiated small airway chip was connected to smoke tubing exiting the smoke machine and the other outlet was connected to the microrespirator. The whole setup fit in a 37°C cell culture incubator. Nine research-grade cigarettes (3R4F; University of Kentucky) were loaded into the moving wheel of the smoke machine, as depicted in Figure S2A. WCS exposure was initiated by the software that controlled and synchronized the breathing-smoking instrument. Key smoking topography parameters we applied were: puff = 2 s; average inter-puff interval = 22 s; 9 cigarettes with 12 puffs/cigarette; inter-cigarette time = 60 s; inhalation time = 2.5 s; exhalation time = 2.5 s; smoke-in time = 1.2 s (150 μL air/smoke volume) at 12 breaths/min. Respiration cycles were 5 s long with 2.5 s for inhalation and exhalation steps. One day following smoke exposure, cells were analyzed for smoke-induced pathologies; the selected breathing and smoking parameters were selected to be representative of what is observed in humans (Lee et al., 2003). A second smoke machine was generated with a slight modification so that its mouthpiece supports loading blu Classic Tobacco-Flavor e-cigarettes (blu eCigs, USA). Every 12 puffs of the e-cigarette was considered equivalent to one full 3R4F tobacco cigarette.

Exposure of Airway Epithelium to Cigarette Smoke Extract in Transwell Inserts

Airway epithelial cells were cultured on Transwell inserts (0.4 μm pore; Corning) under an air-liquid interface. Following differentiation to ciliated epithelium, culture medium (Promocell) with (1, 2 or 4% v/v) or without diluted cigarette smoke extract (CSE) was added apically and incubated for 24h at 37°C before cilia beat analysis. CSE was prepared fresh by combusting 2 X 3R4F cigarettes (University of Kentucky) and bubbling the mainstream smoke through 5 mL of DMEM cell culture medium (Life Technologies). This was subsequently sterilized by passing through a 0.22 μm filter and defined as 100% CSE, and all CSE preparations were used within 20 min after being generated.

Scanning and Transmission Electron Microscopy

Electron microscopic analysis was performed as previously described (Benam et al., 2016). In brief, cells were fixed in 2.5% glutaraldehyde (Electron Microscopy Sciences, USA) for 60 min at room temperature, rinsed with 1% sodium cacodylate and subsequently treated with 1% osmium tetroxide (Electron Microscopy Sciences; USA) for 90 min. Following sequential dehydration in ethanol

gradients, fixed cells were rinsed in hexamethyldisilazane (Sigma), air-dried overnight and then mounted on a conductive carbon support for imaging with a VEGA III scanning electron microscope (Tescan, Czech Republic).

Quantitative RT-PCR

Cells were lysed in situ and total RNA was extracted using RNeasy Mini Kit (QIAGEN). The RNA was treated with DNase I (QIAGEN, USA) for 15 min at RT, incubated at 65°C for 5 min, and then reverse transcribed into cDNA using SuperScript Reverse Transcriptase III kit (Invitrogen) as previously described (Benam et al., 2016). Quantitative PCR was carried out using QuantStudio 7 Flex Real-Time PCR System (Life Technologies). For each reaction, 2 μl cDNA, 10 μl 2 × Universal SYBR Green Supermix (Bio-Rad) and 3 μl of forward and reverse primers (300 nM final concentration), and 2 μl molecular biology-grade water were thoroughly mixed. PCR was performed over an initial cycle at 95°C for 5 min, followed by 45 cycles of 95°C for 5 s and 60°C for 30 s. Cycle of threshold (Ct) values were extracted, and results were analyzed comparatively using $2^{-\Delta\Delta Ct}$ method by normalizing against housekeeping gene hypoxanthine phosphorribosyltransferase (HPRT) as previously described (Benam et al., 2011). In details, first ΔCt for each gene (e.g., $\Delta C_{HMOX1} = Ct_{HMOX1} - Ct_{HPRT}$) was calculated, and then ΔΔCt was established by subtracting ΔCt of non-smoking from ΔCt of smoking condition. Calculating $2^{-\Delta\Delta Ct}$ then generated fold change in gene expression of smoking chips versus non-smoking chips. Primers sequences are listed in the key resources table in STAR Methods.

Microarray Analysis

Total RNA from four chips per condition was extracted as above and submitted to the Dana Farber Microarray Core for analysis using Affymetrix Human ST 2.0 arrays/ The results obtained were robust multi-array average (RMA) data normalized and assessed for quality using Affymetrix Power Tools, and then further processed and analyzed using custom scripts in MATLAB; duplicate genes and data lacking gene IDs were removed prior to analysis. Each smoke-exposed condition was compared to donor-matched non-exposed chips, and genes with both a Student's t test p value < 0.05 and a fold change ≥ 2 were identified for both non-COPD and COPD donor chips to generate lists of significant genes. For differential gene expression, means were subtracted and standard deviations were error propagated. The non-COPD significant gene list was used to compare our small airway chip data with clinical data from bronchoscopic sampling of 10 smokers and 12 non-smokers obtained from the GEO: GSE4498 (Harvey et al., 2007). Smoking samples were normalized to each gene's mean non-smoking control value for both in vitro and clinical data. Heatmaps were generated using clustering linkages based on mean Euclidean distance for both biological samples and individual genes. DAVID software (Huang da et al., 2009) was used to further break down the significant gene lists into functional processes with p values < 0.05. p values were corrected for multiple sampling using the Benjamini-Hochberg correction method.

Analysis and Statistics of Ciliary Beat Frequency

We measured cilia beat frequencies by applying Fourier spectral analysis to bright field video recordings of the ciliated surface. Using an inverted transmission microscope, the ciliated surfaces were recorded at 190-200 frames per second and at 512 × 512 pixel resolution. Each ciliated chip was recorded at 5 to10 fields of view (FOV), each spanning 166 × 166 μm^2. To extract ciliary beat frequencies from these movies, we first identified regions of ciliary motion by calculating the standard deviation of brightness at each pixel over time. High values correspond to notable dynamic changes in pixel brightness, indicating motion and hence ciliary beating (Figure S5A). Next, areas with ciliary motion were thresholded and sampled randomly once per 10 μm^2 (Figure S5B), resulting in a map of ciliary beat frequency at single cell resolution (Figure S5C). At each sample point, average ciliary beat frequency was determined from the time-dependent pixel brightness of up to 300 neighboring pixels, with each pixel's signal reflecting the periodicities of the ciliary movement (Figure S5D). After applying a bandwidth filter of 1 to 30 Hz to remove noise, a Hamming window to reduce sampling artifacts, and Fast Fourier Transform to convert the temporal signal to the frequency domain, the resulting frequency power spectra were averaged to detect one or two dominant frequencies per sample point (Figure S5E). Then, for each FOV, the average ciliary beat frequency was computed for all sample points, resulting in 5 to 10 data points per chip. 'Frequency' in Figures 3B and 4B is equivalent to the number of analyzed FOVs, which in turn, was proportional to the area and optical accessibility of ciliated tissue on the chip. Specifically, we moved the microscope view along on the chip and recorded every FOV that revealed visible cilia and which was amenable to automated image processing. Whereas the number of control and smoked chips mostly matched, tissue and chip properties often changed in response to experimental manipulation, which led to varying numbers of analyzed FOVs per chip. In our studies, we blindly pooled all the video recordings of all chips of the same condition.

For statistical analysis of ciliary beat frequencies across different chip conditions, we first tested whether the measured values of each condition followed normal distributions by using the Shapiro-Wilk Test (alpha level 0.05). To compare the dispersion of sample sets, we used the non-parametric Ansari-Bradley Test to test for inequality of population variance (alpha level 0.05). This test assumes similar medians, and thus, in cases where this condition was not fulfilled, we first equalized medians by subtracting the median value from each dataset.

Western Blot Analysis

Whole cell extracts were lysed with RIPA buffer (50mM Tris-HCl, 150mM NaCl, 1% NP-40, 0.5% sodium deoxycholate, 0.1% SDS), fractionated by SDS-PAGE and transferred to a nitrocellulose membrane using a transfer apparatus according to the manufacturer's protocols (Bio-Rad). After incubation with 5% nonfat milk in TBST (50mM Tris-HCl, 150mM NaCl, 0.1%Tween-20) for blocking, the membrane was incubated with rabbit anti-Nrf2 (phosphor S40) antibody (Abcam), rabbit anti-Nrf2 antibody (Abcam), or mouse

anti-GAPDH antibody (Millipore). A horseradish peroxidase-conjugated goat anti-rabbit or mouse antibody was then added, and membrane was developed with the ECL Plus system (GE Healthcare) according to the manufacture's protocol.

Analysis of Chemokines and Cytokines

The effluent of flowing medium was analyzed for IL-8 and MMP-1 using custom Milliplex assay kits (Millipore, USA). Analyte concentrations were determined according to the manufacturer's instructions, using a LuminexFlexMap 3D system coupled with a Luminex XPONENT software (Luminex, USA).

QUANTIFICATION AND STATISTICAL ANALYSIS

Microarray and CBF statistical analyses are detailed in the respective methods sections above. All other results and error bars are presented as mean standard error of the mean (SEM). Data were analyzed with an unpaired *Student's t test* using Excel software (Microsoft). Differences between groups were considered statistically significant when $p < 0.05$ ($^{*}p < 0.05$, $^{**}p < 0.01$, $^{***}p < 0.001$). The number of replicates for each experiment is specified in figure legends.

DATA AND SOFTWARE AVAILABILITY

Data Resources

The accession number for the transcriptomic data reported in this paper is GEO: GSE87098.